

# EFFECTIVENESS OF VARIOUS VARIANTS OF ELECTRODYNAMIC TREATMENT OF AMg6 ALLOY AND ITS WELDED JOINTS

L.M. LOBANOV, N.A. PASHCHIN, O.L. MIKHODUJ, A.V. CHERKASHIN, A.N. MANCHENKO, I.P. KONDRATENKO and A.V. ZHILTSOV

E.O. Paton Electric Welding Institute, NASU, Kiev, Ukraine

Influence of various variants of discharge circuits on effectiveness of electrodynamic treatment (EDT) of aluminium alloy AMg6 and its welded joints was studied. It is established that maximum EDT effectiveness is achieved at simultaneous impact of pulsed electric current and dynamic load on the treated metal, while minimum effectiveness is achieved at the impact of just the pulsed current. Deformation wave parameters were studied at EDT of AMg6 alloy welded joints.

**Keywords:** *welded joints, aluminium alloy, residual stresses, electrodynamic treatment, deformation wave, flat inductor, capacitive energy storage, treatment effectiveness*

Methods of treatment of metallic materials and their welded joints by applying pulsed electromagnetic fields to them are becoming ever wider accepted at regulation of the stressed state of welded structure elements [1, 2].

One of such methods is electrodynamic treatment (EDT) based on simultaneous impact of electric current and dynamic load on the electric contact point. Electrodynamic impact on the metal (welded joint) is produced at discharge of capacitive energy storage through electric contact of working electrode with the metal surface. Investigations were conducted earlier on evaluation of the influence on treatment effectiveness of such parameters of electrodynamic impact, as charging voltage, storage capacitance, and amplitude values of pulsed current [3]. During current discharge passage electric pulse and dynamic processes are initiated in the treated material, determined by electroplasticity mechanism [4] and generation of deformation waves in the material, respectively. Interaction of electroplastic and dynamic components of EDT at passage of pulsed current through the treated item determines its effectiveness.

The objective of this work is assessment of electroplastic effect and dynamic force load, determining the effectiveness of EDT of AMg6 aluminium alloy and its welded joints.

The work was performed using an EDT system, the principle of operation of which is described in [5], and design features of discharge circuit elements providing the electrodynamic

impact on the treated metal are given in [3]. The system (Figure 1, *a*) consists of capacitive storage  $C$ , flat inductor  $L$ , electrode 2 and disc 3 from nonferromagnetic material. Electric power in the storage device  $C$  in the form of a current pulse is transferred into treated metal 1 at the moment of closing of contactor  $K$ . At current passage through inductor  $L$  a pulsed magnetic field is excited in it, which induces eddy current in the disc. Its interaction with the magnetic field generates an electromagnetic force. Force impact is transferred from the disc to the electrode, which transfers the electrodynamic impact to the metal. Thus, the capacitive storage discharge ensures interaction of two mechanisms — dynamic force impact of the electrode with simultaneous passage of pulsed electric current through the material being treated.

Influence of various variants of discharge circuit (Figure 1) on parameters of electrodynamic impact at EDT was studied, including amplitude values of pulsed current  $I$  and dynamic loads  $P$  during the time of capacitive storage discharge. Measurements of  $I$  and  $P$  were performed in the instrumentation complex, the principle of operation of which is set forth in [3]. Values of pulsed current  $I$  were recorded by contactless method of Rogowski loop, parameters of dynamic load  $P$  were recorded by a piezoelectric pressure sensor, and a cylindrical sample from an aluminium alloy was used as the treated material.

Four circuit variants were studied. In the first (basic) variant (see Figure 1, *a*) discharge current flowed through inductor  $L$ , disc 3, electrode 2 and treated metal 1. In this case, parameters  $I$  and  $P$  were determined by electrodynamic interaction of such circuit elements as «inductor +

disc» and «electrode + metal». In the second variant (Figure 1, *b*), inductor *L* was removed from the disc to distance  $h = 10$  mm, but was included into the circuit. This eliminated the factor of dynamic pressure of the inductor on the disc at preservation of equality of discharge circuits (see Figure 1, *a, b*). In the third variant inductor *L* was completely excluded from discharge circuit (Figure 1, *c*) that allowed assessment of the influence of its resistance on values of parameters *I* and *P*, as well as their rise speeds. The circuits embodied in variants shown in Figure 1, *b, c* allow assessment of the influence of pulsed current on electrodynamic impact at EDT. In the fourth variant (Figure 1, *d*) discharge circuit was closed to inductor *L* that eliminated current flowing through treated metal and allowed assessment of the contribution of dynamic load *P* resulting from interaction of «disc + electrode» elements of the circuit to electrodynamic impact at EDT.

Calculation of parameters *I* and *P* (Figure 2) was conducted by the procedure of [6] at implemented variants of discharge circuit, shown in Figure 1. Figure 2, *a* gives calculated values of pulses of current and load at discharge of capacitive storage of 6600 μF capacitance charged up

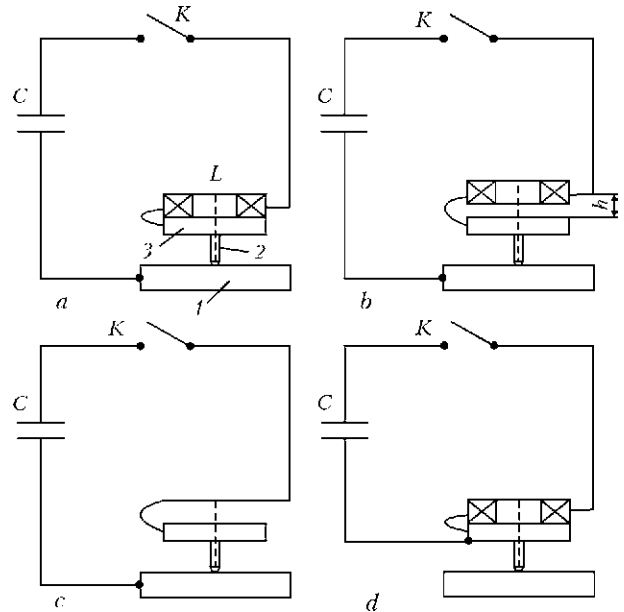


**Figure 1.** Variants of discharge circuit in EDT system: *a* – current discharge runs through flat inductor *L*, disc 3, electrode 2 and metal sample 1; *b* – similar to *a*, but air gap *h* is provided between flat inductor and disc; *c* – current discharge runs through the disc, electrode and metal sample, flat inductor is eliminated; *d* – current discharge runs through the flat inductor and disc

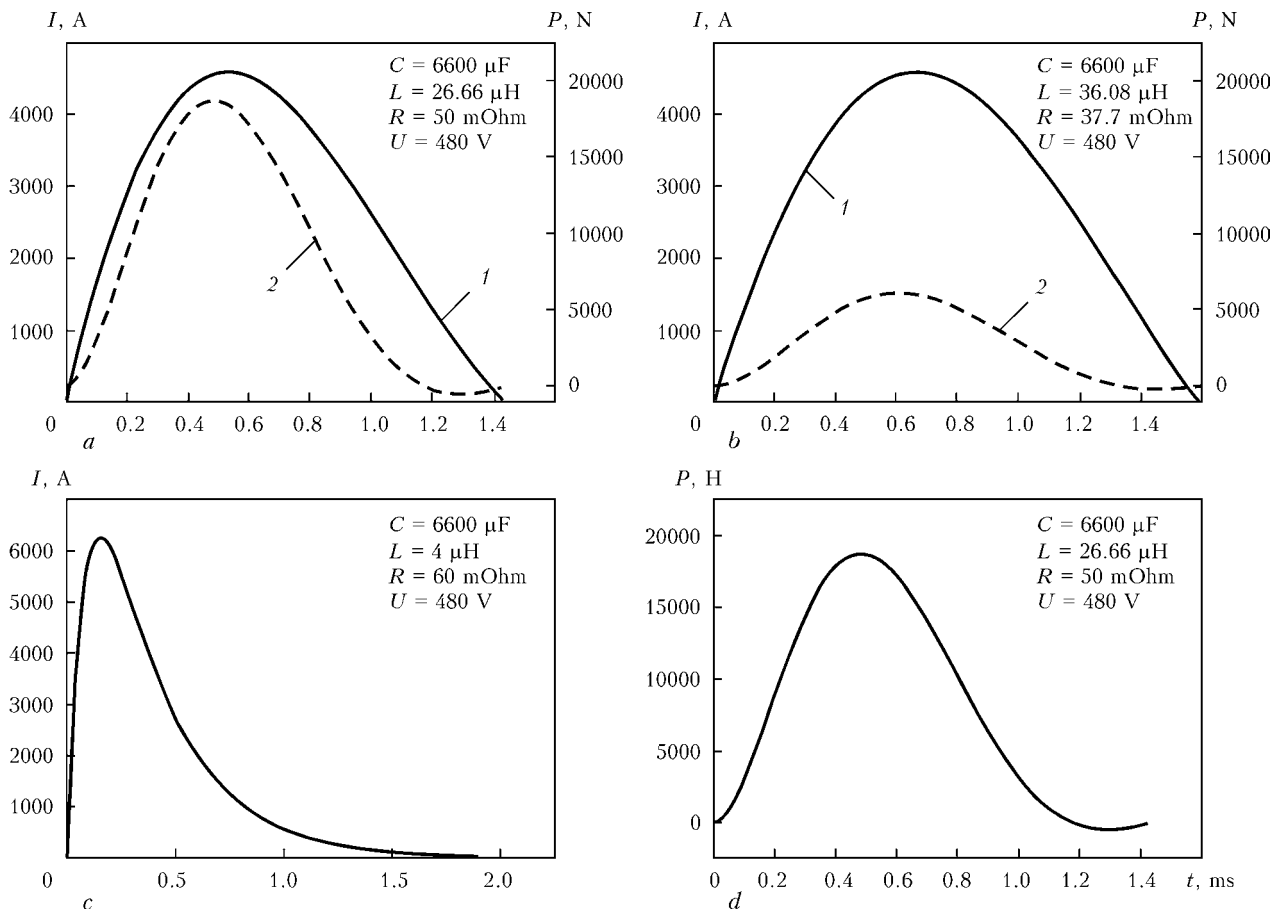


**Figure 2.** Calculated values of pulsed current *I* (1) and dynamic load *P* (2) for discharge circuit variants shown in Figure 1, *a-d*, respectively

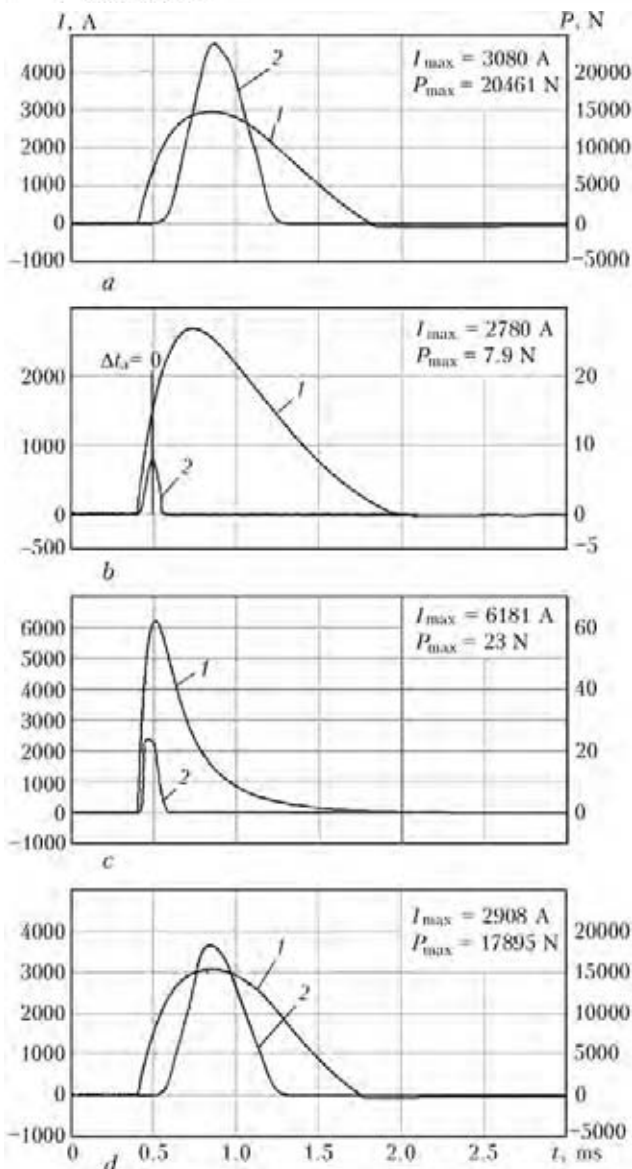


**Figure 3.** Experimental values of pulsed current  $I$  (1) and dynamic load  $P$  (2) at different variants of discharge circuit shown in Figure 1,  $a-d$ , respectively

to 480 V voltage, to inductance of 22.66  $\mu\text{H}$  mounted in the electrode system with a minimum gap between the coil and disc that corresponds to the circuit in Figure 1,  $a$ . It is seen from the Figure that dynamic load reaches its maximum value before current has reached its highest value. This ratio changes only slightly at increase of inductance from 26.66 to 36.08  $\mu\text{H}$ , obtained by increasing the gap between the coil and disc (Figure 2,  $b$ ) that corresponds to the circuit in Figure 1,  $b$ . It should be noted that at any values of capacitance and inductance the maximum calculated value of dynamic load is achieved before current has reached its highest value.

Calculated values of current and load, reached at capacitive storage discharge by the circuits shown in Figure 1,  $c, d$  are given in Figure 2,  $c, d$ , respectively. At removal of inductor from the

discharge circuit, the current pulse is formed by storage capacitance and parasitic inductance of wires, assumed to be equal to 4  $\mu\text{H}$  in calculations, and reaches its maximum value at 6200 A at the moment of time of 0.125 ms. Leading edge of the pulse is shortened approximately 4 times, compared to the variant shown in Figure 2,  $a, b$ , while the dynamic load pulse is absent. Contrarily, when current passage through the treated metal is eliminated at minimum gap between the disc and inductance, a dynamic load is created (Figure 2,  $d$ ) reaching its maximum at 18,000 N at 0.5 ms duration (inductance  $L$  is equal to 26.66  $\mu\text{H}$ ). The amplitude does not differ from the variant shown in Figure 2,  $a$ .

Investigations of the influence of various discharge circuits on parameters  $P$  and  $I$  were conducted at the value of charging voltage  $U$  of capacitive storage device, equal to 480 V. Total capacitance of storage battery of EVOX RIFA 2200 model, included into the discharge circuit, was 6600  $\mu\text{F}$ . Error of measured parameters of electrodynamic impact did not exceed 5%.

Experimentally derived oscillograms of pulsed current  $I$  and dynamic load  $P$  at different variants of discharge circuit are given in Figure 3. Figure shows that when basic circuit (see Figure 1,  $a$ ) was used and just the dynamic load (see Figure 1,  $d$ ) was applied,  $I_{\max}$  values were in the range of 2908–3080 A (Figure 3,  $a, d$ ), which can be assumed to be close. Experimental values of  $I_{\max}$  are below the calculated values, that is attributable to contact resistances of discharge circuit elements, allowing for which is a rather complicated task, going beyond the scope of this study. On the other hand, if maximum value of dynamic load  $P_{\max}$  for basic variant (Figure 1,  $a$ ) was equal to 20,461 N (Figure 3,  $a$ ), for the variate in which the treated material is excluded from discharge circuit and subjected to just dynamic loading (Figure 1,  $d$ ),  $P_{\max}$  did not exceed 17,895 (Figure 3,  $d$ ) that is by 15% lower than the basic one. Experimental  $P_{\max}$  values are quite close to calculated values that is seen from Figure 2,  $a, d$ . Increased values of  $P_{\max}$  for the circuit shown in Figure 1,  $a$ , compared to Figure 1,  $d$ , are attributable to simultaneous electrodynamic impact on the treated metal of such discharge circuit elements as «inductor + disc» and «electrode + metal». In the variant shown in Figure 1,  $d$ , action of «inductor + disc» pair is eliminated and metal is exposed to the impact of just the dynamic load. Periods of the time of impact of parameters  $I$  and  $P$  on the metal for the two considered variants of the circuit were compara-

ble and did not exceed 1.42 and 0.87 ms, respectively (see Figure 3, *a, d*).

A different pattern of distribution of  $I$  and  $P$  values was observed in the absence of dynamic load in those variants of the circuit, when inductor was removed to a distance from the disc (see Figure 1, *b*), as well as completely eliminated from the circuit (see Figure 1, *c*). Periods of action of pulsed current  $I$  in the considered circuit variants were close to calculated ones of 1.6–1.8 ms (see Figure 3, *b, c*), but in the absence of the inductor maximum value of current amplitude  $I_{\max}$  was higher, and the speed of its rise and drop was steeper, that can be seen at comparison of curves 1 in Figure 3, *b, c*, as well as calculated curves (Figure 2, *b, c*). If at inductor removed from the disc (see Figure 1, *b*) maximum current value  $I_{\max}$  was equal to 2780 A, then at its elimination from the circuit  $I_{\max}$  value was 6181 A that is close to the calculated value. This is attributable to lower circuit resistance, because of the absence of inductance element. Speeds of current rise and drop in the case of a distanced inductor (Figure 1, *b*) were 8687 and 2138 A/ms, respectively, and at its elimination from the circuit (see Figure 1, *c*) they were 61,810 and 4578 A/ms. Thus, decrease of the considered circuit inductance and storage device energy, respectively, leads to an increase of the speed of pulsed current rise by more than 7 times, and that of its drop – by more than 2 times. Maximum values of dynamic loads  $P_{\max}$  in the variants of inductor removed to a distance and its elimination reached 7.9 and 23 N, respectively, while the period of their action was 0.16 ms (Figure 3, *b, c*, curves 2). Values of speeds of  $P$  rise/drop in Figure 3, *b* (corresponds to the circuit in Figure 1, *b*) were equal to 79 N/ms, and for the circuit in Figure 3, *c* (corresponds to the circuit in Figure 1, *c*) they were 255 N/ms, that corresponds to  $P_{\max}$  values for the considered circuit variants.

At implementation of circuit variants shown in Figure 1, *b, c* (dynamic load is absent), electrodynamic impact is determined by «electrode + metal» pair. In this case, maximum values of pulsed current  $I_{\max}$ , initiating the electroplasticity mechanisms, correspond to dynamic loads  $P = 0$  at inductor  $L$  placed at a distance from the disc (see Figure 3, *b*, curves 1, 2) and  $P = 0.5P_{\max}$  with inductor eliminated from the circuit (see Figure 3, *c*, curves 1, 2). This results in earlier impact of dynamic load  $P_{\max}$  relative to current  $I_{\max}$  at electrodynamic impact, that is in agreement with calculations (Figure 2, *b, c*).

At comparison of periods of time  $t(I_{\max})$  and  $t(P_{\max})$ , corresponding to maximum values of current and load on curves 1 and 2 (see Figure 3,

*a, d*), a difference from calculated curves is found (Figure 2, *a, d*), expressed in delaying of dynamic load impact  $P_{\max}$  relative to current load  $I_{\max}$ . Calculated and experimental values of speeds of  $P$  rise and drop for circuit variants shown in Figure 1, *a, d*, were equal to 37,000 and 40,000 N/ms, respectively, that shows that at the above-mentioned electrical parameters of the circuit the actual load rise is comparable with the calculated values. It should be noted that real ratios of  $P_{\max}$  and  $I_{\max}$  in the time scale (Figure 3, *a, d*) provide synchronizing of the components of electrodynamic impact on the treated material. Delaying of real rise of dynamic load  $P$  compared to the calculated value is related to plastic deformation of the treated surface at its contact interaction with the spherical tip of the electrode at the moment of capacitive storage discharge.

For a more detailed evaluation of electrodynamic impact on the effectiveness of EDT process, treatment was applied to pre-stretched flat samples of aluminium alloy AMg6 and its welded joints with working area dimensions of  $150 \times 30 \times 4$  mm. Samples were loaded in the rupture machine of «rigid» type with maximum tensile force of 98,000 N at deformation rate of 0.1 mm/s and temperature of 293 K. EDT was performed by series of five current discharges at pulse ratio of 60 s in the mode, taken for investigations of discharge circuit variants (see Figure 3).

Influence of electrodynamic impact on lowering of material resistance to deformation,  $\Delta\sigma$ , was evaluated at different variants of the circuit. Initial value of tensile stress  $\sigma_0$  was taken equal to 150 MPa, at which, according to the data of [7], maximum values of EDT effectiveness –  $\Delta\sigma/\sigma_0$  – are achieved at the above-mentioned mode parameters.

Three variants of discharge circuit were used (Figure 4). In the first variant (Figure 4, *a*) EDT effectiveness was determined by interaction of such circuit elements as «inductor + disc» and «electrode + metal sample». In the second variant of the circuit (Figure 4, *b*)  $\Delta\sigma/\sigma_0$  values were determined by electrodynamic interaction of element pair of «electrode + metal samples», and in the third variant (Figure 4, *c*) – by electrodynamic interaction of «inductor + disc» elements.

Values  $(\Delta\sigma/\sigma_0) \cdot 100$  % after EDT of samples of AMg6 alloy and its welded joints, implemented with different variants of discharge circuit, are shown in Figure 5, from which it is seen that action of just the pulsed current (curves 1 and 1' correspond to the circuit in Figure 4, *b*)

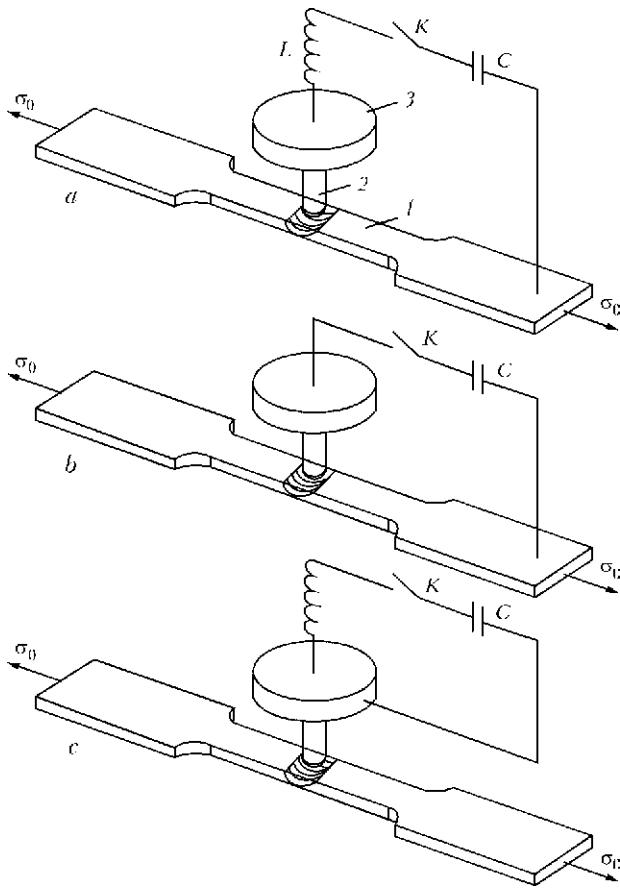


**Figure 4.** Circuits of EDT of AMg6 alloy and its welded joints (for a-c see the text)

does not have any significant influence on deformation resistance, and, consequently, on EDT effectiveness. At comparison of  $(\Delta\sigma/\sigma_0) \cdot 100\%$  values, resulting from EDT under the conditions of dynamic load (curves 2 and 2' correspond to

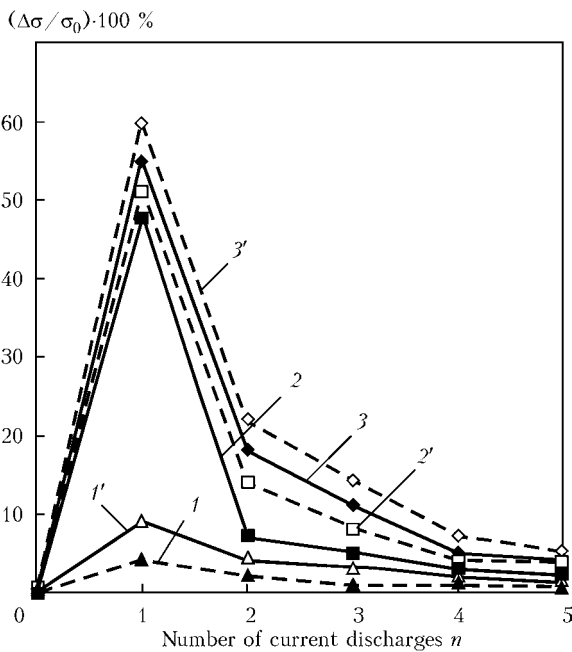


**Figure 5.** Influence of discharge circuit on relative effectiveness of EDT  $(\Delta\sigma/\sigma_0) \cdot 100\%$  of AMg6 alloy and its welded joints (for designations see the text)

the circuit in Figure 4, c), and at interaction of pulsed current and dynamic load (curves 3 and 3' correspond to the circuit in Figure 4, a), one can see that EDT effectiveness at dynamic load has lower values. EDT of base metal is less effective compared to EDT of welded joints that is seen from comparison of curves 1-3 and 1'-3'. This is related to presence of residual stresses in welded joint samples, and in [7] it is shown that effectiveness of electrodynamic impacts depends on values of elastic tensile stresses in the material, subjected to EDT.

Increase of EDT effectiveness at interaction of current and dynamic components, compared to dynamic load, is attributable to interaction of conduction electrons with dislocation clusters during the action of current pulse [8]. Dynamic load, value of which at the above-given charging voltage is equal to 20,460 N, creates the conditions for dislocation clusters overcoming the barriers. Pulsed current provides dislocation displacement by the electron flow at its impact on the metal. Thus, the impact of just the pulsed current without the influence of dynamic load is capable of unpinning the dislocation clusters from stoppers in the material microvolume, but is insufficient for initiating a jump of stresses  $\Delta\sigma$  over the entire cross-section of the sample (Figure 5, curves 1 and 1'). Dynamic load (Figure 5, curves 2 and 2') promotes dislocation clusters overcoming the barriers over the entire section of the sample during the first current discharge ( $n = 1$  in Figure 5), but its effectiveness essentially decreases at subsequent discharges. This is attributable to the fact that at  $n = 1$  the dynamic impact energy ensures overcoming of barriers for dislocation clusters of finite density. The metal preserves stable dislocation groups, the density of which exceeds the energy capabilities of dynamic load that makes low-effective the current discharges  $n = 2-5$  in Figure 5. At the same time, dynamic impact is characterized by the required potential for dislocation unpinning from the stoppers, but is insufficient for their displacement. This assumption is supported by the difference in effectiveness data in the sections of curves 2-2' and 3-3' at  $n = 2-5$  in Figure 5. Pulsed current promotes displacement of dislocations unpinning from the stoppers by dynamic load at  $n = 2-5$  that enables exceeding  $(\Delta\sigma/\sigma_0) \cdot 100\%$ . This is seen at comparison of curves 3-3' and 2-2'. If dynamic load does not provide dislocation unpinning from the stoppers after the first current discharge ( $n = 1$ ), then curves 2-2' and 3-3' coincide during the entire treatment cycle, i.e. at  $n = 1-5$  in Figure 5. Thus, pulsed current is

not the only parameter determining EDT effectiveness. This mechanism is described in [9] for the case of jump-like deformation of aluminium.

For evaluation of dynamic loads initiated by electrodynamic impact, distribution of longitudinal deformation waves was studied at different variants of the discharge circuit corresponding to those shown in Figure 4, *a*, *b*. Investigations were performed using a flat sample of welded joint of AMg6 alloy, on the surface of which a strain gauge with 10 mm base was placed along the central longitudinal axis at 70 mm distance from the center of the sample, the surface of which was treated by single current discharge in the mode corresponding to charging voltage of 480 V. Sensor readings were recorded with two-channel digital oscillograph PCS Welleman at 0.1 ms scan.

Values of deformation waves  $\varepsilon_{EDT}$  initiated by dynamic load (without current impact) and electrodynamic impact are given in Figure 6. From the Figure one can see that maximum range of wave amplitude, which is equal to 0.0042, corresponds to electrodynamic impact (curve 2). No residual plastic deformation was recorded in the strain gauge measurement zone. This is confirmed by the results given in [7], where it is stated that the region of plastic deformation at EDT is localized in the zone of electrodynamic impact.

As is seen from Figure 6, the periods of rise of primary deformation wave for the two variants of the circuit, are equal to each other, being 0.05 ms. Here, the speed of deformation wave rise at dynamic load (curve 1) is equal to 0.04 ms, and at electrodynamic impact (curve 2) it reaches 0.049 ms. Higher speed of wave rise achieved under the conditions of current flowing through the sample, ensures maximum values of tensile deformations of 0.0024 (curve 2). At sample exclusion from discharge circuit stress value was not higher than 0.002 (curve 1). More noticeable is the influence of pulsed current in the flat region of primary wave drop, where the difference of values of tensile deformations on curves 1 and 2 was up to 0.0007 during 0.12 ms.

Results of conducted investigations lead to the conclusion that pulsed current treatment has the smallest influence on lowering of residual

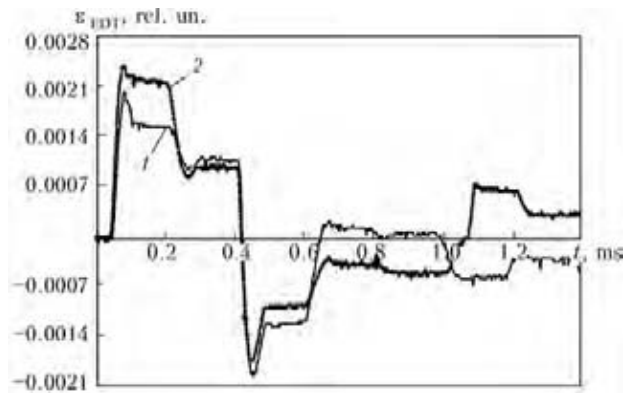


Figure 6. Values of deformation waves  $\varepsilon_{EDT}$  initiated by dynamic load (1) and electrodynamic impact (2)

stresses in welded joints of AMg6 alloy. More effective is the impact of dynamic load realized without pulsed current passage through the treated material. The highest effectiveness of EDT is found at pulsed current passage through the material, at its simultaneous action with the dynamic load on samples with welded joint. Thus, such an impact is preferable at EDT of welded joints of sheet structures from aluminium alloys.

1. Lobanov, L.M., Pashchin, N.A., Loginov, V.P. et al. (2005) Application of electric pulse treatment of structural elements to extend their service life (Review). *The Paton Welding J.*, **11**, 19–23.
2. Stepanov, G.V., Babutsky, A.I., Mameev, I.A. et al. (2011) Redistribution of residual welding stresses after treatment by pulsed electromagnetic field. *Problemy Prochnosti*, **3**, 123–131.
3. Lobanov, L.M., Pashchin, N.A., Cherkashin, A.V. et al. (2012) Efficiency of electrodynamic treatment of aluminium alloy AMg6 and its welded joints. *The Paton Welding J.*, **1**, 2–6.
4. Baranov, Yu.V., Troitsky, O.A., Avramov, Yu.S. et al. (2001) *Physical principles of electric pulse and electric plastic treatments and new materials*. Moscow: MGIU.
5. Lobanov, L.M., Pashchin, N.A., Skulsky, V.M. et al. (2006) Influence of electrodynamic treatment on the stress-strain state of heat-resistant steels. *The Paton Welding J.*, **5**, 8–11.
6. Aleksandrov, G.N. (1985) *Theory of electric apparatuses*. Moscow: Vysshaya Shkola.
7. Lobanov, L.M., Pashchin, N.A., Loginov, V.P. et al. (2007) Change of the stress-strain state of welded joints of aluminium alloy AMg6 after electrodynamic treatment. *The Paton Welding J.*, **6**, 7–14.
8. Strizhalo, V.A., Novogrudsky, L.S., Vorobiov, E.V. (2008) *Strength of materials at cryogenic temperatures taking into account the action of electromagnetic fields*. Kiev: IPP.
9. Bobrov, V.S., Lebedkin, M.A. (1989) Electric effects at low-temperature jump deformation of aluminium. *Fizika Tv. Tela*, **31(6)**, 120–124.